Characterization of electrochemical systems using Potential Step Voltammetry. Part I: Modeling by means of Equivalent Circuits.

J.E. Ramón[1,2], A. Martínez-Ibernón[1,2], J.M. Gandía-Romero[1,2], R. Fraile[4], R. Bataller[1], M. Alcañiz[1,3], E. García-Breijo[1,3] and J. Soto[1].

[1]Interuniversity Research Institute for Molecular Recognition and Technological Development (IDM), Universitat Politècnica de València, Universitat de València

[2]Department of Architectural Construction, Universitat Politècnica de València

[3]Department of Electronic Engineering, Universitat Politècnica de València

[4]Research Center for Software Technology and Multimedia Systems for Sustainability (CITSEM). Universidad Politécnica de Madrid

Corresponding Autor: M. Alcañiz

Abstract

Potential step voltammetry is used to characterize the resistive and capacitive properties of electrochemical systems. Within those systems, electrochemical processes are modeled by means of equivalent circuits (ECs). In this study, we established and experimentally validated algebraic expressions describing the electrical response of those ECs. We then analyzed the features that allow significant differentiation between the ECs. Finally, we have proposed a method to graphically visualize and analyze the electrical response of the circuit to a potential step sequence. The application of this method to real electrochemical systems will allow us to not only identify the electrochemical processes taking place in an experiment but to also assess parameters such as the double layer

capacitance, the solution resistance, and the polarization resistance of the redox process.

Keywords: *potential step voltammetry, modeling, equivalent circuits.*

1. Introduction

The study of interfacial activity in metal-solution systems is of great interest due to its potential applications in science and technology. Some examples include the optimization of the capacitive deionization process of water [1], improvement in the design of electrolytic capacitors for storing energy, improvement in techniques employed in the electropolishing of metal surfaces (electronic tongue treatment) [2], [3], and environmental applications such as electrocatalytic carbon dioxide reduction [4].

However, despite the practical importance of these fields of application and all the effort dedicated to them, advances in the last 50 years have uncovered theoretical and practical difficulties [5]. Even so, studies on the interfacial phenomenon have not lost momentum, and several authors, such as Delahay [6], Devanathan [7], Parsons [8], and Schmickler [9] have worked to expand our knowledge and improve the basic elements of these systems.

The first model was established by Helmholtz who, when studying electrolytic solutions, proved that the electrical behavior of the metal-solution interface was similar to that of electrical capacitors. Therefore, he proposed that the interfacial response in these systems could be modeled with this type of electrical component [10]. Between 1910 and 1913, Gouy and Chapman developed and

proposed the “diffuse layer model,” in which they argued that the capacitive effects were due to the metal interacting with the statistical distribution of charge caused by electrostatic interactions and thermal agitation. Unfortunately, neither of the two theoretical models fit the measured values with acceptable precision.

In 1924, Stern proposed the electrical “double layer model,” which was the result of combining the Helmholtz rigid layer model with the Gouy-Chapman diffuse layer model. Stern proposed that the double layer would behave similarly to two capacitors connected in series.

Scientists are exploring new methodologies for modeling the theoretical behavior of the interfacial region such as those based on ab initio [11] quantum mechanics or on density-functional theory (DFT). Both of these models have been used to study the adsorption processes of typical anions such as Cl^-, SO_4^{-2}, or PO_4^{-3}, whose distributions depend on the electric potential applied. These anions are adsorbed on specific areas of the metal surface and are separated by solvent molecules, although occasionally some cations such as K^+ or Na^+ adsorb on those surfaces [12]. This type of theoretical calculation helps us understand the ion-solvent-electrode interactions and therefore expands our knowledge on interfacial processes and their theoretical basis.

In recent years, a large part of our work has been dedicated to the study of the electronic tongue based on pulse voltammetry and its application to different areas of technological interest such as, for example, quality control of water, drinks, and food. In a recent study we discussed the importance of the geometric design of measuring cells and the electropolishing of electronic tongue electrodes [13], [14] to implement automatic “on-line” control systems. Despite the efforts of

different research groups to fit the intensity values obtained in voltammetric electronic tongue measurements to existing equivalent circuits [15], [16], according to our experience there are still some discrepancies that could be overcome by making some modifications to these equivalent circuits. As a consequence of those recent results, we present this paper, in which we outline an approach to modeling the metal-solution interface.

2. Experimental

For all subsequent analyses, the modeled electrochemical system will consist of an electrochemical cell with an inert electrolyte solution, where two electrodes made of the same material are inserted (e.g. two Au electrodes). If there is a significant difference in their surfaces, it makes it so the working electrode (e.g. a microelectrode) is ideally polarizable while the counter electrode is not.

2.1 Potential step sequence design

The behavior of the systems was studied when a sequence of potential steps $v(t)$ was applied. A graph of such sequence is depicted in Fig. 1. The open-circuit potential (OCP) is marked as V_0, and this is the initial potential. The amplitude of all subsequent potential steps is denoted as ΔV_j, and t_j is the time at which each step happens. The overpotential value corresponding to each step is referred to as η_j. Both the potential steps and the overpotential values are illustrated in **Figure 1**. Apart from the definitions of ΔV_j and η_j given in **Figure 1**, note that the following relations are also true:

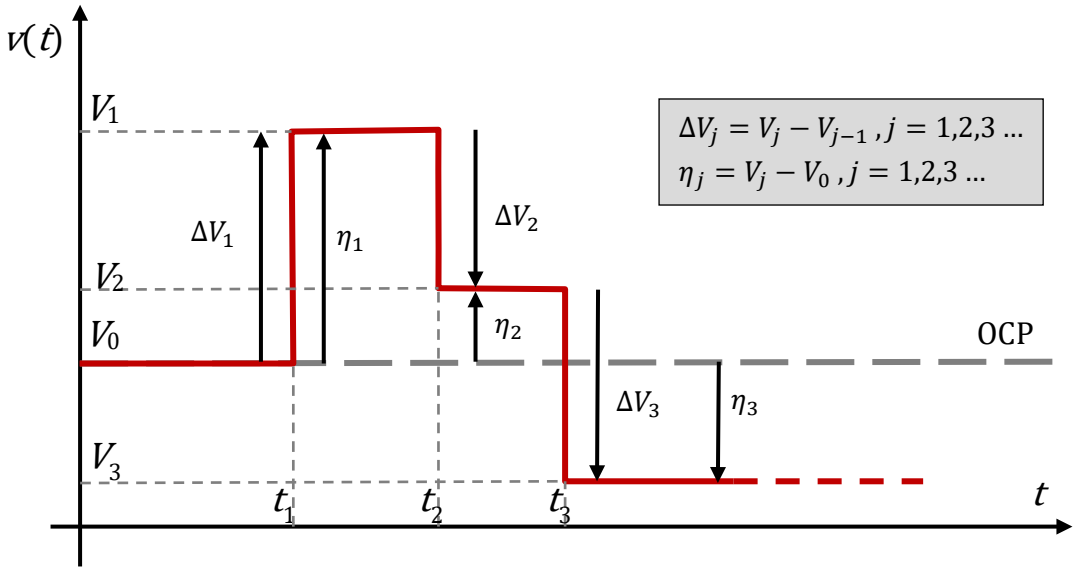

Figure 1. Potential steps sequence diagram and relationship between the overpotential and potential values.

- Each potential step can be expressed as the difference between the following overpotential and the one prior to it:

$$\Delta V_j = \eta_j - \eta_{j-1} \tag{1}$$

- Each overpotential value can be calculated as the cumulative sum of the previous potential steps:

$$\eta_j = \sum_{k=1}^{j} \Delta V_k \tag{2}$$

We employed potential step voltammetry to experimentally validate the algebraic expressions obtained for the electrical response of each one of the equivalent

circuits. Six circuits with different values for resistors and capacitors were evaluated for each EC.

In most cases, the basic prerequisite we required of the potential step sequence design was that after applying a complete potential step cycle, the net charge accumulated in the system had to be zero or negligible. This could be accomplished if the charge started from an initial OCP and returned to the same value at the end, while the intermediate steps had symmetrical potential and time duration. On the other hand, the step duration had to be long enough for the exponentially decaying terms to vanish before the next potential was applied. The duration of the potential steps $\Delta t = t_j - t_{j-1}$ was evaluated based on the time constant of the system ($R_s C_{dl}$ or $\frac{R_s R_p}{R_s + R_p} C_{dl}$, depending on the models). The pattern sequence designed included four potential steps, distributed symmetrically with respect to the OCP (V_0) value. The following steps were employed: the sweep started at V_0 and, once the duration of the pulse Δt had passed, the following potential step was applied while recording the variation in current intensity. After a time, again equal to Δt, the cell returned to V_0 and stayed for another time interval, Δt. The third potential step was applied in the direction opposite to the first one. Last, another potential step was applied to return the cell to the OCP value. Thus, the values of the variables referred to in **Figure 1** were as follows:

$$t_j = j\,\Delta t \qquad j = 1, 2, 3, 4 \tag{3}$$

$$\eta_1 = \Delta E \quad \eta_2 = 0 \quad \eta_3 = -\Delta E \quad \eta_4 = 0 \tag{4}$$

$$\Delta V_1 = \Delta E \quad \Delta V_2 = -\Delta E \quad \Delta V_3 = -\Delta E \quad \Delta V_4 = \Delta E \tag{5}$$

We repeated each of the scans five times and averaged the measurements obtained before employing those numbers in later calculations. To study the

reproducibility of the measurements, the basic potential step sequence proposed can be sequentially repeated twice, hence making the total number of potential steps equal to eight.

We experimented with several amplitudes ΔE for the potential steps in order to test the analytical reproducibility of the equivalent circuits studied.

2.2 Equivalent circuits measurements

All the measurements were performed in a Faraday cage with the aim of electrically shielding the system. For the validation studies on the various equivalent circuit models proposed, we used standard resistors and capacitors. Resistive and capacitive elements were assembled without soldering (by inserting the component in a breadboard). Although the values indicated in the paper are the nominal values of the components, the values used in the calculations were obtained using a FLUKE 28 II multimeter.

The equipment used to perform the potential step voltammetry assays were the Autolab PGSTAT 100 and a potentiostat FRA-Plus-Mini, which has previously been described in the literature [16].

3. Theory

3.1 General structure of the equivalent circuit

Equivalent circuits are useful in electrochemical studies in order to understand and interpret, and later to predict the behavior of the systems [17]. Using them allows us to obtain an electrical response similar to that of the electrochemical

system that is being studied when a voltammetric or a specific amperometric boost is applied.

Figure 2 shows the general structure of the equivalent circuit of an electrochemical system. The left-most voltage generator represents the sequence of potential steps forced upon the system, that is, the function $v(t)$ in **Figure 1**. The electrochemical system itself comprises a battery providing a continuous voltage V_0 equal to the OCP, and a linear circuit whose composition will depend on the specific theoretical models for the interfacial processes being studied, though it usually includes discrete electrical components: resistors, inductors, capacitors, etc. Note that the inclusion of the battery is necessary if the OCP is to be modeled, since a purely linear circuit cannot account for this effect.

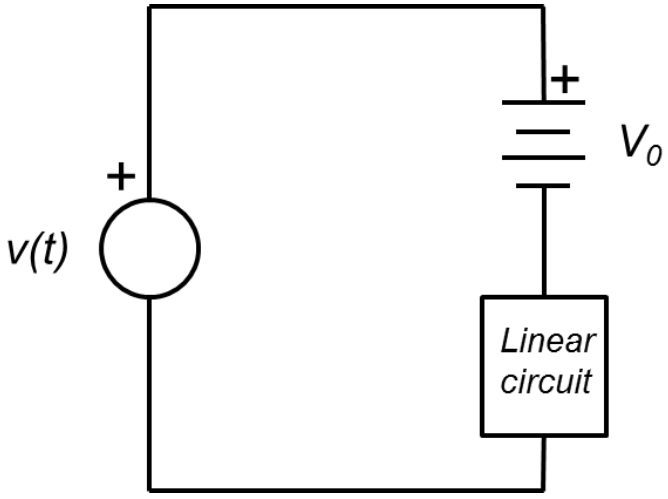

Figure 2. General structure of the equivalent circuit of an electrochemical system.

3.2 Faradaic and non-Faradaic processes

Electrodic processes are traditionally classified as either Faradaic or non-Faradaic. The current in non-Faradaic processes is associated with electric charging and discharging processes at interfacial regions. For these physical processes, the transported charge depends on the magnitude of the potential

step applied (ΔV_j) [18]. This is an important factor that must be taken into account when attempting to carry out an accurate study of the double electric layer and its electrochemical properties.

On the other hand, Faradaic processes are associated with electron transfer through the metal-solution interface, so redox processes occur. The electrokinetic model of Butler and Volmer established the basis for the theoretical model of this type of current exchange. According to their model, the current transferred is a function of the overpotential (η_j) applied.

Given that both phenomena can and usually do take place simultaneously in electrodic processes, it would be logical that any mathematical model that tries to accurately interpret the electrochemical behavior of these systems would include not only the potential step difference but also the overpotential applied. A general equation for this is the following:

$$i_j(t) = i_{\mathrm{NF}}(\Delta V_j; t) + i_{\mathrm{F}}(\Delta V_j, \eta_j; t) \tag{6}$$

Where $i_j(t)$ is the total current that goes through the system at any time between the j^{th} and $(j+1)^{\text{th}}$ voltage steps; $i_{\mathrm{NF}}(\Delta V_j; t)$ is a function that models the non-Faradaic component of such current; and $i_{\mathrm{F}}(\Delta V_j, \eta_j; t)$ is the function that models the Faradaic component.

Eq. 3 can also be written as a function of overpotentials:

$$i_j(t) = i_{\mathrm{NF}}(\eta_j - \eta_{j-1}; t) + i_{\mathrm{F}}(\eta_{j-1}, \eta_j; t) \tag{7}$$

However, this aspect is not usually taken into account in fundamental theoretical models or in the most commonly used equations in electrochemistry because the

theoretical modeling of electrochemical processes is truly complex. This difficulty is the main reason why for this type of study it is ideal to find a situation in which only one process type (Faradaic or non-Faradaic) is the dominant one. For example, in some transient analysis techniques such as voltammetry and polarography, the signal is not recorded during the first moments of measuring in order to minimise the weight of non-Faradaic currents that appear mainly at the beginning of the transient.

In many cases, the simplifications used to address the modeling of electrochemical processes allow us to achieve results that are consistent with the experimental data. Unfortunately, there is a negative side to this type of simplification, since it does not allow us to obtain a global vision of the process. Electrochemical techniques are usually dynamic. Therefore, if the simultaneous existence of Faradaic and non-Faradaic processes is not taken into account, we may misinterpret the electrochemical behavior of the systems or miscalculate their properties.

3.3 Modeling non-Faradaic electrochemical processes with equivalent circuits

To analyze what happens in the electrode-solution system when an electrical boost is applied, we can use the diagram shown in **Figure 3**, where the two branches involved in an electrodic system are shown. These branches are:

1. The electronic branch, which goes from the equipment that generates the current signal through a conductor wiring to the electrodes.
2. The ionic branch, which is associated with the solution where the current movement is in parallel (according to Kohlrausch's law of independent

migration of ions). For this reason, the number of branches for the ionic conduction depends on the number of different existing ions.

If a potential difference is applied to this system, ions begin to migrate toward the electrodes in order to compensate for the electrical charge gradient created. Capacitance phenomena and Faradaic processes are found in the region between the electrodes and the solution. The movement of charge between the solution and the interfacial regions will not stop until electrostatic equilibrium is achieved with respect to the imposed electric field.

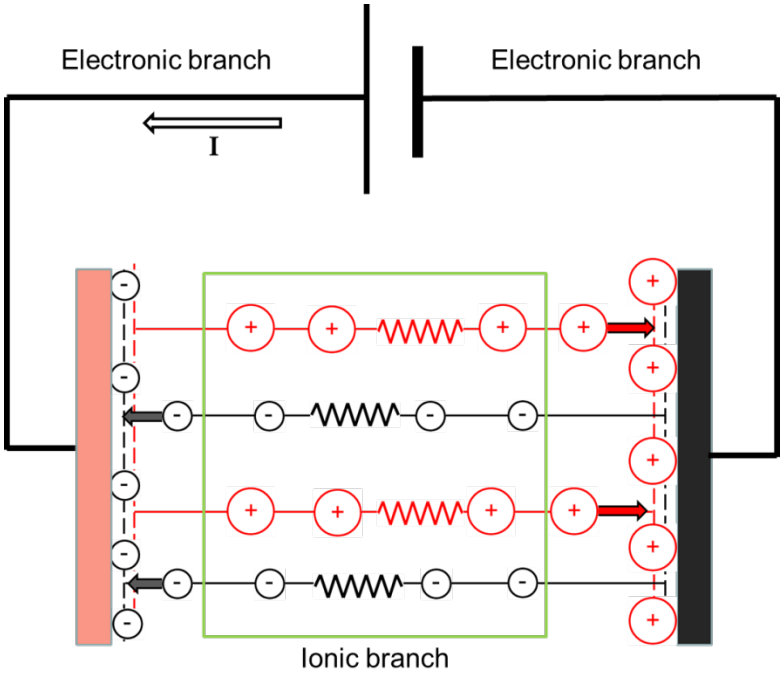

Figure 3. Diagram for the interpretation of non-Faradaic processes, when a direct current is applied between two electrodes.

In **Figure 3**, the discontinuous lines parallel to the electrodes represent the approximation limit of anions and cations to the electrode surface. The distance from these electrical double layers to each electrode depends on the type of ion and its ionic radius, and on the solvation and temperature of the system. The total

charge accumulated at the interface between the working and counter electrodes allows the electrical capacity of the system to be calculated. If we know the electrical potential of each electrode in the final steady state.

On the other hand, the independent migration principle of Kholrausch requires at least two resistors in parallel to be inserted, one associated with the movement of cations in the solution and the other with the anions.

3.3.1 Randles Equivalent Circuit

Figure 4-A shows the Randles equivalent circuit, which can be used when working with potential steps to explain the non-Faradaic processes shown in **Figure 3**. This circuit corresponds to the "linear circuit" block in **Figure 2**. The electrical conduction from the ions contained in solution is associated with R_{s+} and R_{s-} resistance, while the interfacial electrical properties of the working and counter electrodes are associated with capacitors C_{dl+} and C_{dl-}.

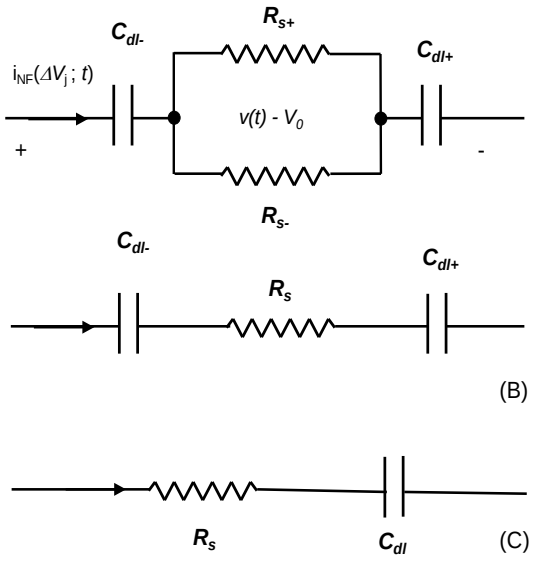

Figure 4. Randles equivalent circuits proposed to study the electrochemical behavior of non-Faradaic systems in solution when applying direct current between two electrodes. (A) Typical EC (B) Simplified EC and (C) Reduced EC.

It is common to use a simplified equivalent circuit (**Figure 4-B**) where the parallel resistors (R_{s+} and R_{s-}) have been replaced by their equivalent resistance R_s:

$$\frac{1}{R_s} = \frac{1}{R_{s+}} + \frac{1}{R_{s-}} \quad (8)$$

However, it is even more common to use a reduced equivalent circuit (**Figure 4-C**), where the capacitors associated with the cathode and anode have been replaced by an equivalent capacitor, C_{dl}:

$$\frac{1}{C_{dl}} = \frac{1}{C_{dl+}} + \frac{1}{C_{dl-}} \quad (9)$$

The theoretical modeling for the reduced Randles circuit response shown in **Figure 4-C** leads to Eq. 10, which gives the current intensity through the RC system caused by a potential step between the two electrodes (see section I in the appendix):

$$i_{NF}(\Delta V_j; t) = \frac{\Delta V_j}{R_s} e^{-\frac{t-t_j}{R_s C_{dl}}} \quad (10)$$

3.3.2 Stern equivalent circuit

The Randles equivalent circuit has been used to analyze experimental data by applying the Helmholtz model as well as the Gouy Chapman model but it has not provided satisfying results. Stern suggested that poor fit between experimental data and simulations using the previous models (**Figure 4**) is due to the simplicity of these models. Aiming to solve those problems, he suggested that each of the

electrodes' charged regions (Helmholtz and Gouy Chapman) acted as a capacitor in series with respect to the electrode surface. According to this suggestion, when non-specific adsorption of ions occurs, the total double-layer capacity formed by the outer Helmholtz plane and the diffuse layer results in the following equation:

$$\frac{1}{C_{\mathrm{dl}}} = \frac{1}{C_{\mathrm{H}}} + \frac{1}{C_{\mathrm{GC}}} \qquad (11)$$

Where C_{dl} represents the electrical double layer capacitance, C_{H} the outer Helmholtz plane capacitance, and C_{GC} the Gouy-Chapman diffuse layer capacitance. Accordingly, the reduced Randles equivalent circuit (**Figure 4-C**) is modified by inserting two capacitors in series, to obtain the Stern model (**Figure 5**).

The introduction of the double condenser proposed by Stern into the basic Randles circuit, leads back to the equivalent circuit presented in **Figure 4-B**, as long as the following relationship between the capacitors forming the electrical double layer is true:

$$\frac{1}{C_{dl}} = \frac{1}{C_{dl+}} + \frac{1}{C_{dl-}} = \frac{1}{C_{H+}} + \frac{1}{C_{GC+}} + \frac{1}{C_{H-}} + \frac{1}{C_{GC-}} \qquad (12)$$

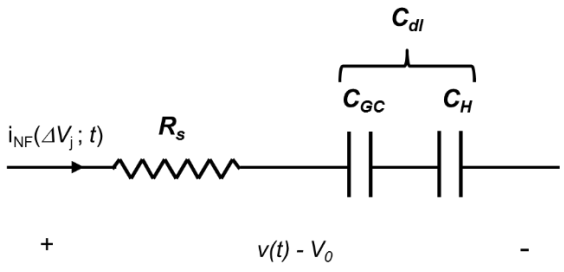

Figure 5. The Reduced equivalent circuit proposed by Stern to study non-Faradaic electrochemical behavior in a solution by applying potential steps between two electrodes.

The equivalence between Randles and Stern models implies that the Stern model cannot provide any improvement with regards to fitting experimental data.

3.3.3 Equivalent circuit for a binary salt system

Based on the Helmholtz rigid layer model, we know that when the electrolyte solution studied contains two different salts (which are inert from the redox point of view), its reduced equivalent circuit has to have two capacitors in parallel. These capacitors are associated with the mixed interface formed by the two types of ions that are in direct contact with the metal surface, both on the cathode and anode. If the number of different ion species is greater than two, it would be necessary to use more capacitors in parallel.

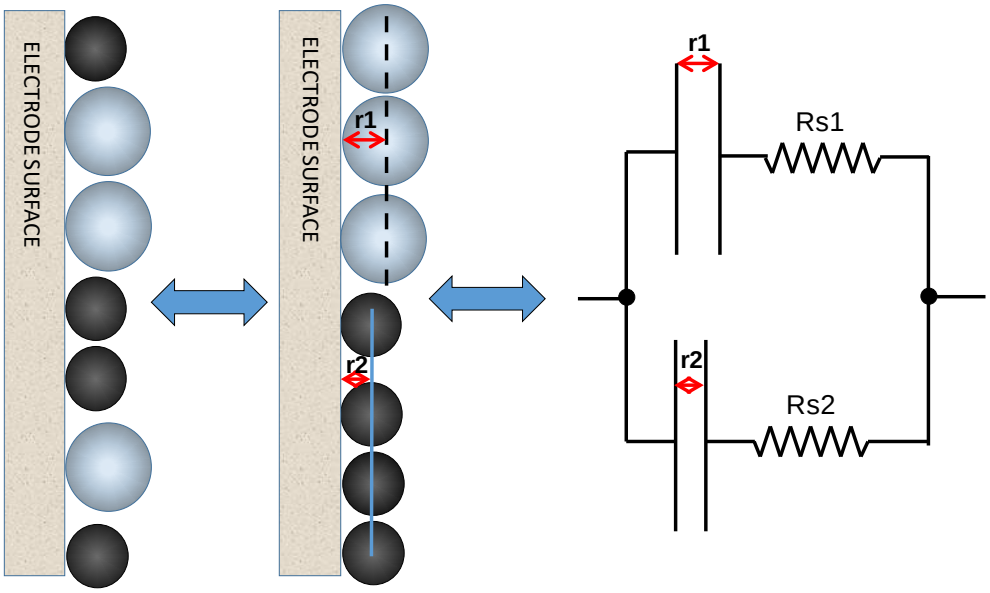

Figure 6. Reduced equivalent circuit (R_{s1}-C_{dl1})//(R_{s2}-C_{dl2}) proposed to study the non-Faradaic electrochemical behavior of a binary salt solution, by applying direct current between two electrodes.

Figure 6 shows two types of ions (i.e., of a different size or charge) physisorbed on the metal interface due to the electrical field, and in random order. If the ions are ordered by size, two different charge levels are clearly established and arranged in a Helmholtz-type configuration, in parallel. The diagram also includes the resistances (R_s), associated with the ion transport for each type of salt present in the system. Therefore, the reduced equivalent circuit corresponding to a binary salt system must be similar to that shown in this figure.

Since the circuit consists of two parallel branches equal to that of **Figure 4-C** and the same potential step is applied to both branches, the current response can be modeled as the sum of two currents in the same way as in Eq. 10:

$$i_{\mathrm{NF}}\left(\Delta V_j; t\right) = \frac{\Delta V_j}{R_{\mathrm{s1}}} e^{-\frac{t-t_j}{R_{\mathrm{s1}} C_{\mathrm{dl1}}}} + \frac{\Delta V_j}{R_{\mathrm{s2}}} e^{-\frac{t-t_j}{R_{\mathrm{s2}} C_{\mathrm{dl2}}}} \tag{13}$$

where R_{s1} and R_{s2} are the values of the resistance associated with ion transport and the capacitors (C_{dl1} and C_{dl2}) are associated with the interfacial capacitance of each salt in Farads.

3.4 Modeling electrochemical Faradaic processes with equivalent circuits

Just as two different cases were presented to study non-Faradaic processes, two possible cases to model Faradaic electrochemical processes can also be considered. The first one is a simple system, where only one redox electrode process occurs at the working electrode, while the second model presents a system with two electrode processes that can occur simultaneously. Extending this model for *n* electroactive species would allow us to interpret the behavior of

complex systems such as, for example, multicomponent systems studied using electronic voltammetric tongues.

3.4.1 Simple Faradaic Systems

The simplest equivalent circuit used for the study of Faradaic electrodic processes is shown in **Figure 7**. The figure represents a reduced equivalent circuit, similar to that shown in **Figure 4-C**, but with a parallel resistance (R_p) added to the capacitor associated with the electrical double layer.

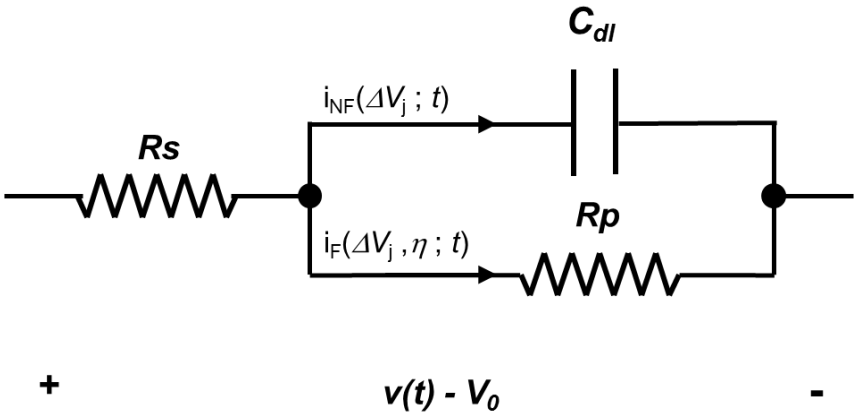

Figure 7. Reduced equivalent circuit R_s-(R_p//C_{dl}) employed to model Faradaic processes when a potential step between two electrodes is applied.

The solution to the differential equation in this model is formed by three terms (see section II in the appendix). The first two are associated with the Faradaic currents that cross the interface because of the resistance (R_p); these include one constant term depending on the overpotential and one decaying term which is a function of the potential step. The third term is associated with the non-Faradaic current accumulated in the C_{dl} capacitor, and it is a decaying term whose amplitude is a function of the potential step too:

$$i_{\mathrm{F}}(\Delta V_j, \eta_j; t) + i_{\mathrm{NF}}(\Delta V_j; t) \tag{14}$$

$$= \frac{\eta_{\mathrm{j}}}{R_p + R_s} - \frac{\Delta V_{\mathrm{j}}}{R_p + R_s} e^{-(t-t_j)\frac{R_p+R_s}{R_p R_{\mathrm{s}} C_{\mathrm{dl}}}} + \frac{\Delta V_j}{R_{\mathrm{s}}} e^{-(t-t_j)\frac{R_p+R_s}{R_p R_{\mathrm{s}} C_{\mathrm{dl}}}}$$

3.4.2 Binary Faradaic systems

A binary Faradaic system is formed by two species (1 and 2) that can be oxidized or reduced at the electrode surface. Both processes are independent of one another, and may take place at the same time if the conditions of the electric potential applied are appropriate. The equivalent circuit diagram intended for application in this type of process consists of two models (see **Figure 7**) in parallel, as shown in **Figure 8**.

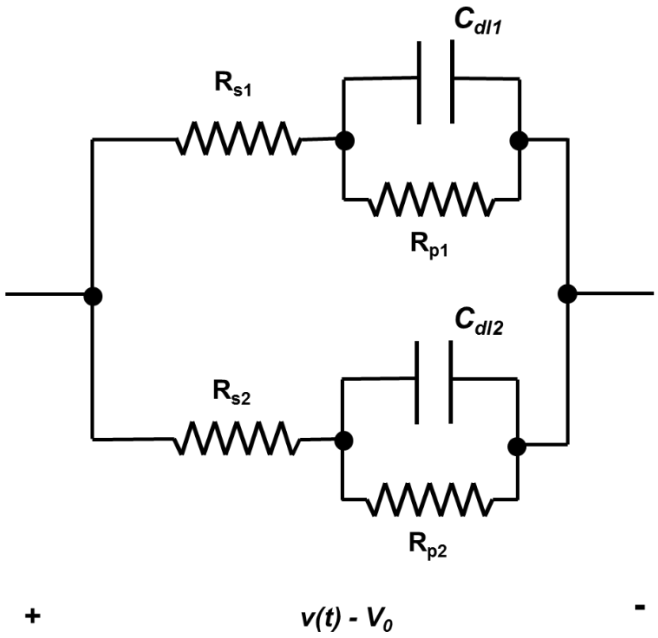

Figure 8. Reduced equivalent circuit (R_{s1}-(R_{p1}//C_{dl1}))//(R_{s2}-(R_{p2}//C_{dl2})) proposed for the study of systems with dual Faradaic processes and continuous current.

From Eq. 14 it is easy to demonstrate that when a potential step is applied, the Faradaic current that passes through this equivalent circuit or, in general, one

with a larger number *N* of branches in parallel (in a similar diagram) results in the following:

$$i_{\mathrm{F}}\left(\Delta V_j, \eta_j; t\right) + i_{\mathrm{NF}}\left(\Delta V_j; t\right) \tag{15}$$

$$= \sum_{n=1}^{N} \left(\frac{\eta_j}{R_{\mathrm{p}n} + R_{sn}} - \frac{\Delta V_j}{R_{\mathrm{p}n} + R_{sn}} e^{-(t-t_j)\frac{R_{\mathrm{p}n}+R_{sn}}{R_{\mathrm{p}n}R_{sn}C_{\mathrm{dl}n}}} \right.$$

$$\left. + \frac{\Delta V_j}{R_{sn}} e^{-(t-t_j)\frac{R_{\mathrm{p}n}+R_{sn}}{R_{\mathrm{p}n}R_{sn}C_{\mathrm{dl}n}}} \right)$$

where the subscript *n* refers to each branch of the system.

3.5 Mixed Faradaic and non-Faradaic systems

One of the most common situations found in electrochemical studies is a system with two different soluble ionic compounds, with the first one being an inert salt from a redox point of view, while the second one is an active redox component. Usually, an inert background salt is used to reduce the solvent resistance and to ensure that the transport of the active redox agent is controlled mainly by diffusion. In this case, the equivalent circuit related to the electrochemical system would be similar to that shown in **Figure 9**. If we apply a potential difference, the inert electrolyte, which is associated with the non-Faradaic branch (formed by R_{s1} y C_{dl1} in series), will transport a non-Faradaic charge (Q_{1nF}), while the electroactive salt associated with the Faradaic branch will transport a fraction of the non-Faradaic charge (Q_{2nF}). The Q_{2nF} will be accumulated in C_{dl2}, and so will a Faradaic charge (Q_{2F}) that passes through the polarization resistance (R_{p2}).

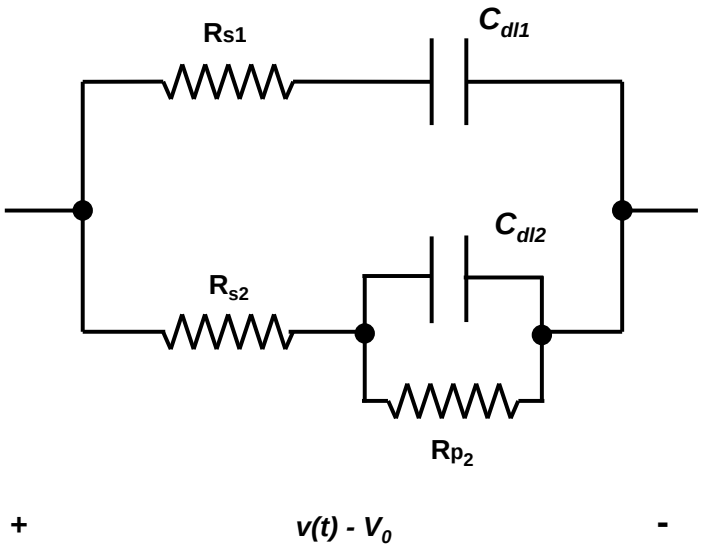

Figure 9. Reduced equivalent circuit (R_{s1}-C_{dl1}))//(R_{s2}-(R_{p2}//C_{dl2})) proposed to study mixed Faradaic and non-Faradaic systems.

The mathematical model that corresponds to the electrical behavior of the previous equivalent circuit results from the sum of Eq. 10 and Eq. 14:

$$i_{\mathrm{F}}\left(\Delta V_j, \eta_j; t\right) + i_{\mathrm{NF}}\left(\Delta V_j; t\right) \tag{16}$$

$$= \frac{\Delta V_j}{R_{\mathrm{s1}}} e^{-\frac{t-t_j}{R_{\mathrm{s1}} C_{\mathrm{dl1}}}} + \frac{\eta_{\mathrm{j}}}{R_{p2} + R_{s2}} - \frac{\Delta V_{\mathrm{j}}}{R_{p2} + R_{s2}} e^{-(t-t_j)\frac{R_{p2}+R_{S2}}{R_{p2} R_{\mathrm{s2}} C_{\mathrm{dl2}}}}$$

$$+ \frac{\Delta V_j}{R_{\mathrm{s2}}} e^{-(t-t_j)\frac{R_{p2}+R_{S2}}{R_{p2} R_{\mathrm{s2}} C_{\mathrm{dl2}}}}$$

4. Results and discussion

4.1 Equivalent circuit models for non-Faradaic processes

4.1.1 Analysis of potential step sequences in an R_s-C_{dl} system

The current intensity response for the whole duration of the pulse sequence of the R_S-C_{dl} system can be obtained from Eq. A.9:

$$i_j(t) = \frac{1}{R_s}\sum_{i=1}^{j} \Delta V_i e^{-\frac{t-t_i}{R_s C_{dl}}} \qquad t_j < t \leq t_{j+1} \tag{17}$$

To study the dynamic response in RC systems when the potential step sequence described by Eqs. 14 to 16 is applied, it can be more convenient to analyze the charge variations accumulated in the capacitor than to try to make a direct analysis of the variations in current intensity. After applying a potential step ΔV_j, the charge (q_j) stored in the capacitor (C_{dl}) can be calculated as in Eq. A.26:

$$q_j(t) = C_{dl}\eta_j - C_{dl} e^{-\frac{t-t_j}{R_s C_{dl}}} \sum_{i=1}^{j} \Delta V_i e^{-\frac{t_j - t_i}{R_s C_{dl}}} \tag{18}$$

Another interesting way to analyze the electrical response of RC networks to a potential step sequence is to calculate the natural logarithm for the absolute value of intensity. From Eq. 17:

$$\log i_j(t) = -\log R_s - \frac{t-t_j}{R_s C_{dl}} + \log\left(\sum_{j=1}^{J} \Delta V_j e^{-\frac{t_j - t_j}{R_s C_{dl}}}\right) \tag{19}$$

For sufficiently long voltage steps, the last term in Eq. 19 can be approximated by ΔV_j:

$$\log i_j(t) = -\log R_s - \frac{t-t_j}{R_s C_{dl}} + \log \Delta V_j = \log\left(\frac{\Delta V_j}{R_s}\right) - \frac{t-t_j}{R_s C_{dl}} \tag{20}$$

Figure 10 shows the electrical response of the R_S-C_{dl} network to the pulse sequence obtained from the experimental measurements and from the application of the algebraic expressions. The duration of each potential step is $\Delta t = 20\ \mathrm{ms}$ while the amplitude is $\Delta E = 1\ \mathrm{V}$.

Figure 10-A shows the difference between the experimental and theoretical transient current. Although by visual inspection a good match between

experimental data and theoretical values is observed, due to the sharp transition at the beginning of each pulse and the low current values at the end, the quantitative validation of this fitting is highly affected by the noise.

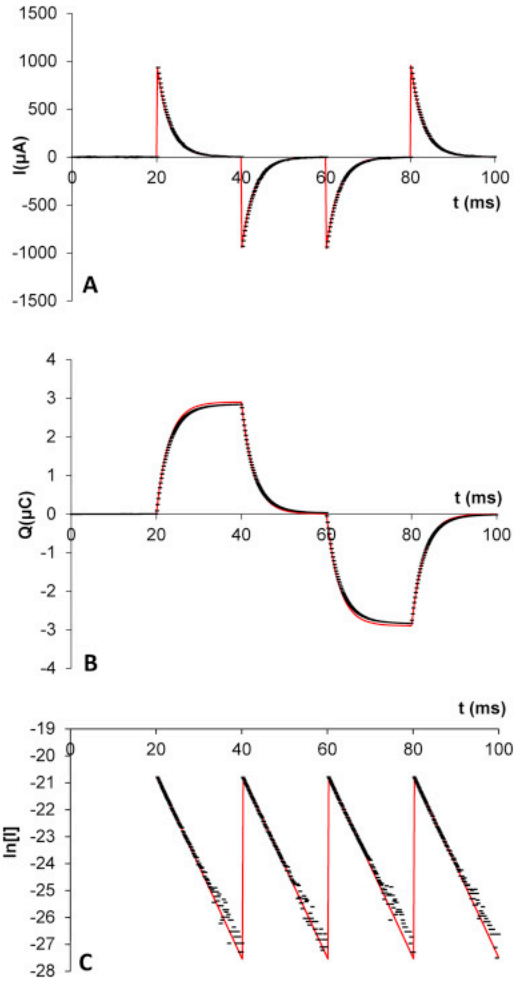

Figure 10. Experimental data of the electrical response of an R_s-C_{dl} network (C_{dl}=3 μF and R_s=1 kΩ) to the potential step sequence (Δt=20 ms and ΔE=1 V). (A) Transient current (B) Accumulated charge (C) Logarithm of the transient current (points in the first interval $\boldsymbol{t < t_1}$ have been omitted because of the erratic values obtained when the measured current was close to zero and therefore affected by electrical noise processes).

Figure 10-B shows the charge stored in the capacitor as a function of time. It is noteworthy that the charge limit is 3 μC and the discharge is practically complete after each of the cycles. The charge signal allows more convenient quantitative

evaluation of the fitting between the experimental data and the theoretical values (Eq. 18) than the current signal. **Table 1** shows the fitting of the normalized root mean square error (NRMSE) obtained for the six configurations tested for this EC. The NRMSE for this study is defined as the root mean square error (RMSE) normalized to the root mean square value of the signal (RMS).

Table 1. Experimental validation of the algebraic expression of the accumulated charge for different R_s-C_{dl} circuits

EC	ΔV (V)	Δt (ms)	R_s (Ω)	C_{dl} (μF)	NRMSE (%)
1	0.3	2	60	3	2.07
2	0.3	2	100	1	4.35
3	0.3	10	100	10	2.75
4	0.3	100	100	100	2.53
5	1	20	1000	3	3.46
6	1	300	1000	39	3.19
EC	ΔV (V)	Δt (ms)	R_s (Ω)	C_{dl} (μF)	NRMSE (%)
1	0.3	2	60	3	2.07
2	0.3	2	100	1	4.35
3	0.3	10	100	10	2.75
4	0.3	100	100	100	2.53
5	1	20	1000	3	3.46

6	1	300	1000	39	3.19

For all the ECs the NRMSE is below 5%. Considering the signal noise and the limited accuracy of the equipment used to apply and measure signals, these low NRMSE values prove that Eq. 18 is suitable for interpreting the electrical behavior of RC systems and could be used to experimentally obtain the values of R_s and C_{dl} in real electrochemical non-Faradaic systems.

Figure 10-C shows the natural logarithm for the absolute value of intensity as a function of time in milliseconds.

Consistent with Eq. 20, the graph in **Figure 10-C** consists of a set of parallel lines starting from a value near -7, since $\ln\left(\frac{1}{1000}\right) \approx -6.9$ (recall that for this experiment $\Delta E = 1\ \mathrm{V}$ and $R_s = 1\ \mathrm{k}\Omega$). The slope of each line, $-\frac{1}{R_s C_{\mathrm{dl}}}$, can be used to estimate the time constant of the system.

Taking into account the results shown in **Figure 10**, the potential pulses composing the sequence defined by Eqs. 14 to 16 can be divided into two groups. The first one, or “excitation steps,” causes the capacitor to become charged, and the second group, or “relaxation steps,” is where the behavior of the system is dominated by the discharge of the capacitor. Therefore, the potential steps corresponding to overpotential transitions from 0 to 1 V and from 0 to -1 V are excitation steps, while the steps corresponding to transitions from 1 V to 0 and from -1 V to 0 are relaxation pulses. The initial null overpotential can be considered a neutral point of charge.

Figure 11 illustrates the electrical response for the same R_s-C_{dl} system but with a step time of only 5 ms. Experimental and theoretical data fit consistently by visual inspection for all three signals.

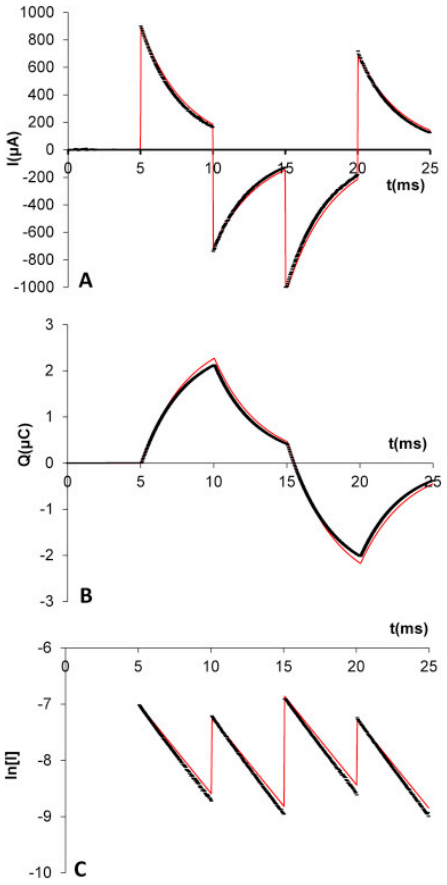

Figure 11. Experimental data of the electrical response of an R_s-C_{dl} network (C_{dl}=3 μF and R_s=1 kΩ) to the potential steps sequence (Δt=5 ms and ΔE=1 V). (A) Transient current (B) Accumulated charge (C) Logarithm of the transient current.

The main differences between **Figure 10-A** and **Figure 11-A** are related to the peak intensity. In **Figure 10-A**, the peak intensity remains practically constant while in **Figure 11-A** it varies significantly because of the reduced pulse duration, which means that the capacitor does not reach its steady state, neither fully charged nor fully discharged, before the application of each potential step. On the other hand, it should be emphasized that when working with two electrodes, the obtained function $i(t)$ relates the intensity directly to time as well as to the overpotential applied (Eq. 17).

Figure 11-B shows the experimental and theoretical (Eq. 18) data fitting of the charge stored in the capacitor as a function of time. As mentioned previously, in this case the value of the charge in the capacitor is not zero at the end of the relaxation pulses.

When the logarithm of the current is plotted (**Figure 11-C**) the start and end points for the parallel lines are now different for each pulse.

4.1.2 Response of the equivalent circuit in binary systems (R_{s1}-C_{dl1})//(R_{s2}-C_{dl2})

The electrochemical intensity-time and charge-time responses of a binary system modeled by two parallel RC branches can be derived from Eqs. 10 and 18:

$$i_j(t) = \frac{1}{R_{\mathrm{s1}}} e^{-\frac{t-t_j}{R_{\mathrm{s1}}C_{\mathrm{dl1}}}} \sum_{i=1}^{j} \Delta V_i e^{-\frac{t_j-t_i}{R_{\mathrm{s1}}C_{\mathrm{dl1}}}} + \frac{1}{R_{\mathrm{s2}}} e^{-\frac{t-t_j}{R_{\mathrm{s2}}C_{\mathrm{dl2}}}} \sum_{i=1}^{j} \Delta V_i e^{-\frac{t_j-t_i}{R_{\mathrm{s2}}C_{\mathrm{dl2}}}} \tag{21}$$

$$q_j(t) = (C_{\mathrm{dl1}} + C_{\mathrm{dl2}})\,\eta_j - C_{\mathrm{dl1}} e^{-\frac{t-t_j}{R_{\mathrm{s1}}C_{\mathrm{dl1}}}} \sum_{i=1}^{j} \Delta V_i e^{-\frac{t_j-t_i}{R_{\mathrm{s1}}C_{\mathrm{dl1}}}} - C_{\mathrm{dl2}} e^{-\frac{t-t_j}{R_{\mathrm{s2}}C_{\mathrm{dl2}}}} \sum_{i=1}^{j} \Delta V_i e^{-\frac{t_j-t_i}{R_{\mathrm{s2}}C_{\mathrm{dl2}}}} \tag{22}$$

Figure 12 illustrates the electrical response of an (R_{s1}-C_{dl1})//(R_{s2}-C_{dl2}) circuit. Although the graph morphology for the transient current (**Figure 12-A**) and the accumulated charge (**Figure 12-B**) for this binary system is very similar to the case of simple systems, the behavior of the $\log i_j(t)$ signal (**Figure 12-C**) presents a clear difference. The decreasing segments have two different slopes: the slope of the first part is inversely proportional to $\min(R_{\mathrm{s1}}C_{\mathrm{dl1}}, R_{\mathrm{s2}}C_{\mathrm{dl2}})$, while it is

inversely proportional to $\max(R_{s1}C_{dl1}, R_{s2}C_{dl2})$ for the second part. Note that all the peaks in the graph have the same amplitude, which corresponds to a situation in which $\Delta t \gg \max(R_{s1}C_{dl1}, R_{s2}C_{dl2})$. Therefore, the current logarithm signal can be used to identify the type of processes taking place in a non-Faradaic experiment.

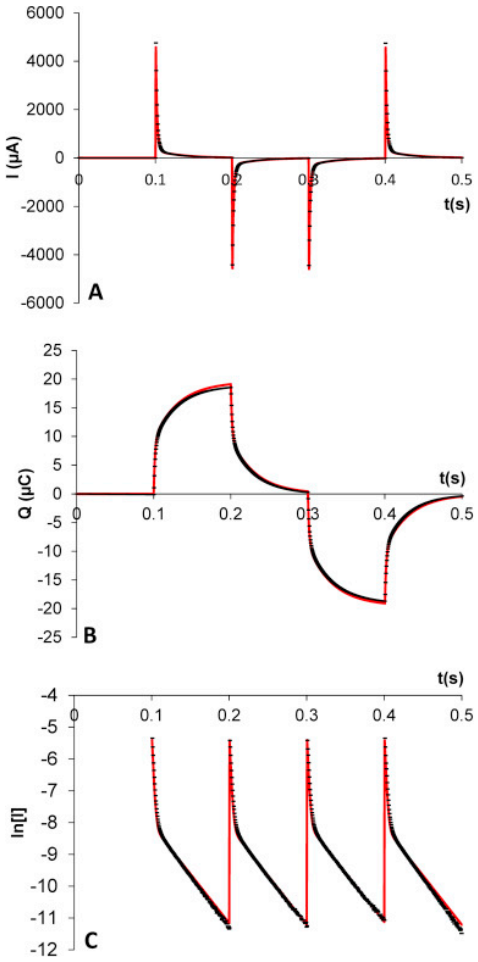

Figure 12. Experimental data of the electrical response of an (R_{s1}-C_{dl1})//(R_{s2}-C_{dl2}) network (C_{dl1}=10 μF, C_{dl2}=10 μF, R_{s1}=3200 Ω and R_{s2}=180 Ω) to the potential steps sequence (Δt=100 ms and ΔE=1 V). (A) Transient current (B) Accumulated charge (C) Logarithm of the transient.

Good agreement between experimental and theoretical data for the algebraic expression of the accumulated charge (Eq. 22) was obtained as shown in **Table 2**.

Table 2. Experimental validation of the algebraic expression of the accumulated charge for different (R_{s1}-C_{dl1})//(R_{s2}-C_{dl2}) circuits

EC	ΔV (V)	Δt (ms)	R_{s1} (Ω)	C_{dl1} (μF)	R_{s2} (Ω)	C_{dl2} (μF)	NRMSE (%)
1	1	200	200	100	500	39	2.92
2	1	100	1000	10	500	10	4.70
3	1	200	1000	10	500	39	3.02
4	1	200	1000	10	500	100	2.73
5	1	100	3200	10	180	10	3.16
6	0.5	500	3200	10	180	100	3.09

4.2 Equivalent circuit model for Faradaic processes

The validity of Eq. 14, which is associated with the reduced equivalent circuit shown in **Figure 7**, is demonstrated by fitting the experimental data obtained from a set of electrical circuits. **Figure 13** shows this typical behavior characteristic of R_s-(R_p//C_{dl}) systems. The morphology of the intensity-time curve has differential features with respect to the same representations of the current response in non-Faradaic systems (**Figure 10** and **Figure 11**). In this case, an anodic and cathodic residual current remains in pulse pairs 1 and 3, but not in the even pulses.

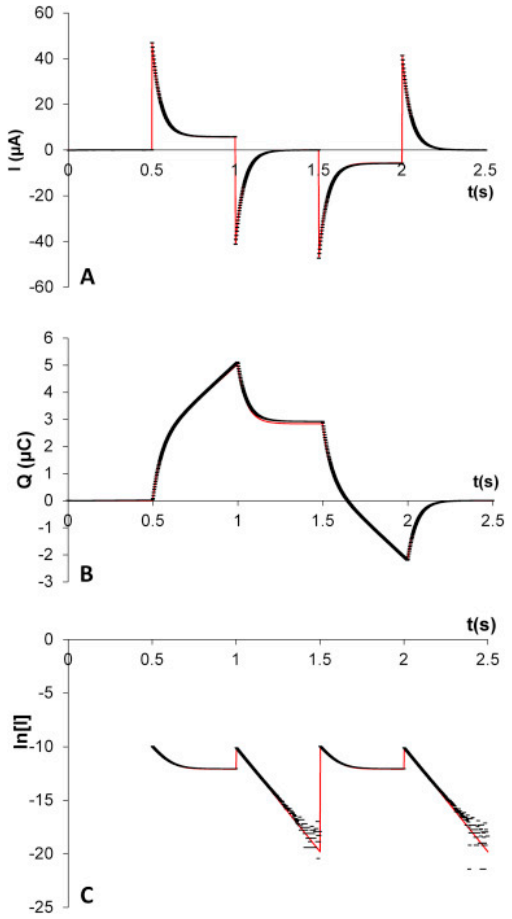

Figure 13. Experimental data for the electrical response of an R_s-(R_p//C_{dl}) network (C_{dl}=10 μF, R_s=6200 Ω and R_p=47 kΩ) to the potential steps sequence (Δt=500 ms and ΔE=0.5 V). (A) Transient current (B) Accumulated charge (C) Logarithm of the transient currents (points in the first interval $\boldsymbol{t < t_1}$ have been omitted because of the erratic values obtained when the measured current was close to zero and therefore affected by electrical noise processes).

The plot of the integrated current for the sequence of potential steps shows a typical morphology, clearly different from the morphology presented for the integral charge curve in pure R_s-C_{dl} and (R_{s1}-C_{dl1})//R_{s2}-C_{dl2}) non-Faradaic circuits. This morphology is described by Eq. A.30:

$$q_j(t) = \frac{\eta_j\left(t - t_j\right)}{R_p + R_s} + \frac{\Delta t}{R_p + R_s}\sum_{i=1}^{j-1}\eta_i + \frac{\eta_j R_p^2 C_{\mathrm{dl}}}{\left(R_p + R_s\right)^2} - \frac{\Delta V_j R_p^2 C_{\mathrm{dl}}}{\left(R_p + R_s\right)^2} e^{-(t-t_j)\frac{R_p+R_s}{R_p R_s C_{\mathrm{dl}}}} \quad (23)$$

The reason is that the first term in Eq. 23 implies a linear dependence between transferred charge and time for a single pulse (*j*=1). When this linear term appears due to a potential step with positive overpotential η_{j} (the first step in **Figure 13**), it cannot be compensated by merely applying a null-overpotential step (second step). Particularizing Eq. 23 for $\eta_1 > 0$ and $\eta_2 = 0$ would result in:

$$q_2(t) = \frac{0 \cdot \left(t - t_j\right)}{R_p + R_s} + \frac{\Delta t}{R_p + R_s}\eta_1 + \frac{0 \cdot R_p^2 C_{\mathrm{dl}}}{\left(R_p + R_s\right)^2} + \frac{\eta_1 R_p^2 C_{\mathrm{dl}}}{\left(R_p + R_s\right)^2} e^{-(t-t_j)\frac{R_p+R_s}{R_p R_s C_{\mathrm{dl}}}} = \frac{\Delta t}{R_p + R_s}\eta_1 + \frac{\eta_1 R_p^2 C_{\mathrm{dl}}}{\left(R_p + R_s\right)^2} e^{-(t-t_j)\frac{R_p+R_s}{R_p R_s C_{\mathrm{dl}}}} \quad (24)$$

which tends to a non-zero constant value. Compensation of the transferred charge would require the application of a potential step with opposite amplitude $-\eta_1$ (third step) followed by an additional step returning to OCP. In Eq. 24, the last term is dominant when $t \gtrsim t_j$, which implies that the behavior of **Figure 13-B** is almost an exponential decay at the beginning of each pulse. However, as *t* grows, the first term (linear) becomes dominant, which is also apparent by the end of each pulse in **Figure 13-B**.

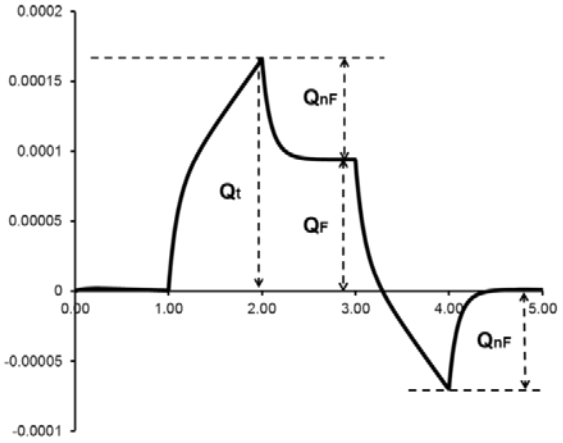

Figure 14. Experimental data of the charge transferred during the potential step transient. It is noteworthy that the charge limit depends on R_p and that the discharge is practically complete after each of the four potential steps.

When the pulse duration is long enough, the plot of accumulated charge as a function of time allows us to graphically determine the value of the capacitance for the capacitor (C_{dl}), the Faradaic charge value transferred in the equivalent circuit, and the total resistance (R_s + R_p). Taking into account the exponentially decaying term in Eq. 24, the value of the capacitance is obtained according to Eq. 25:

$$C_{dl} = \frac{Q}{\Delta V_c} = \frac{Q}{\Delta V} \cdot \left(1 + \frac{R_s}{R_p}\right)^2 \tag{25}$$

The value of R_s + R_p is obtained according to Eq. 14. The required parameters are the potential step, the pulse duration, and the Faradaic charge value obtained from **Figure 14**.

Table 3 summarizes the NRMSE values obtained in the experimental validation of the algebraic expression of the accumulated charge (Eq. 23) for different R_s-(R_p//C_{dl}) circuits.

Table 3. Experimental validation of the algebraic expression of accumulated charge for different R_s-(R_p//C_{dl}) circuits

EC	ΔV (V)	Δt (ms)	R_s (Ω)	C_{dl} (μF)	R_p (Ω)	NRMSE (%)
1	0.3	1000	100	1000	550	1.76
2	0.3	2000	6200	100	4700	1.46
3	0.3	800	100	100	4700	1.11
4	0.3	500	6200	10	47000	2.44
5	0.3	5000	6200	100	47000	2.72
6	0.3	8000	6200	100	470000	3.85

As for non-Faradaic circuits, the low NRMSE values validate the use of Eq. 23 to experimentally assess the value of R_s, R_p, and C_{dl} in Faradaic experiments.

Figure 13-C shows the absolute value of the logarithm of the total current, for each of the transients versus time. The graph obtained shows a very different morphology compared to the plots associated with pure non-Faradaic processes (**Figure 10**). The peaks in **Figure 10** are still observed, but those associated with excitation steps are preceded by segments with almost vertical slope, which can be noticed if the time resolution of measurements is appropriate. In the relaxation steps, the plot is not flat even when $\log I_J(t)$ is less than -13. This is due to residual current effects, combined with electrical noise.

Therefore, the representation of charge versus time is very useful in order to calculate the resistance value in parallel (R_p). A disadvantage that could occur is that the zero current does not fit perfectly, causing a linear drift of the charge to take place (positive or negative depending on the offset value), although this effect can be easily compensated if detected.

4.3 Equivalent circuit model for mixed Faradaic and non-Faradaic processes

Figure 15 shows the transient current, accumulated charge and current logarithm signals for an (R_{s1}-C_{dl1})//(R_{s2}-(R_{p2}//C_{dl2})) network.

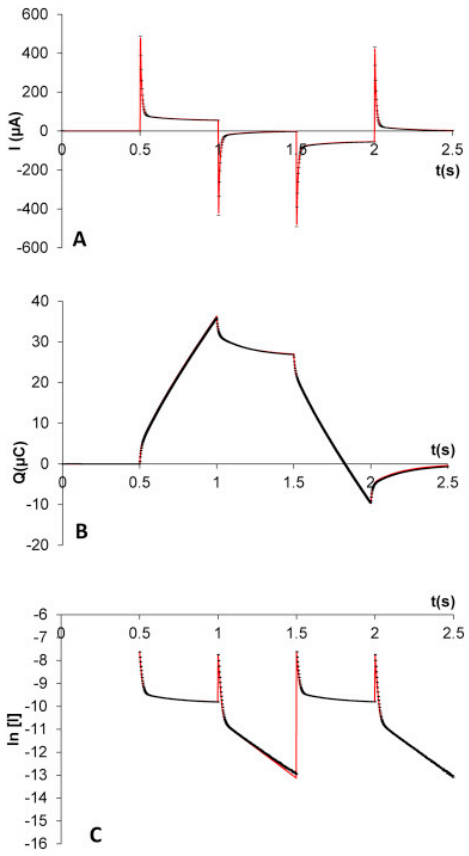

Figure 15. Experimental data of the electrical response of an (R_{s1}-C_{dl1})//(R_{s2}-(R_{p2}//C_{dl2})) network (C_{dl1}=10 µF, C_{dl2}=100 uF, R_{s1}=1000 Ω, R_{s2}=6200 Ω and R_{p2}=3200 Ω) to the potential steps sequence (Δt=500 ms and ΔE=0.5 V). (A) Transient current (B) Accumulated charge (C) Logarithm of the transient current.

The experimental validation of the algebraic expression of the accumulated charge (a combination of Eq. 18 and Eq. 23) for different (R_{s1}-C_{dl1})//(R_{s2}-(R_{p2}//C_{dl2})) networks is shown in **Table 4**. As for the previous systems, the low NRMSE values justify the use of the accumulated charge as a reliable tool to obtain the double layer capacitance, the solution resistance, and the polarization resistance in real electrochemical experiments.

Table 4. Experimental validation of the algebraic expression of the accumulated charge for different (R_{s1}-C_{dl1})//(R_{s2}-(R_{p2}//C_{dl2})) circuits

EC	ΔV (V)	Δt (ms)	R_{s1} (Ω)	C_{dl1} (μF)	R_{s2} (Ω)	C_{dl2} (μF)	R_{p2} (Ω)	NRMSE (%)
1	0.5	200	100	10	560	100	3200	1.98
2	0.5	10	560	3	100	10	3200	2.84
3	0.5	700	1000	10	6200	100	3200	1.66
4	0.5	500	1000	10	6200	100	3200	1.49
5	0.5	1000	1000	100	1000	100	3200	1.46
6	0.5	400	6200	10	1000	10	3200	0.68

4.4 Proposed methodology

Figure 16 shows the intensity-time response, the charge-time response, and the logarithm of the absolute value of intensity versus time for the most significant equivalent circuits. The plots show that Faradaic and non-Faradaic processes are easily distinguishable if they are compared by looking at the $\log I_J(t)$ diagram.

Simple, double, or multiple non-Faradaic circuits have similar morphology (linear or piecewise linear with equal amplitude of current). Faradaic circuits have different currents for excitation and relaxation pulses, with a linear appearance in relaxation pulses and curvilinear morphology when the system is mixed (Faradaic + non-Faradaic).

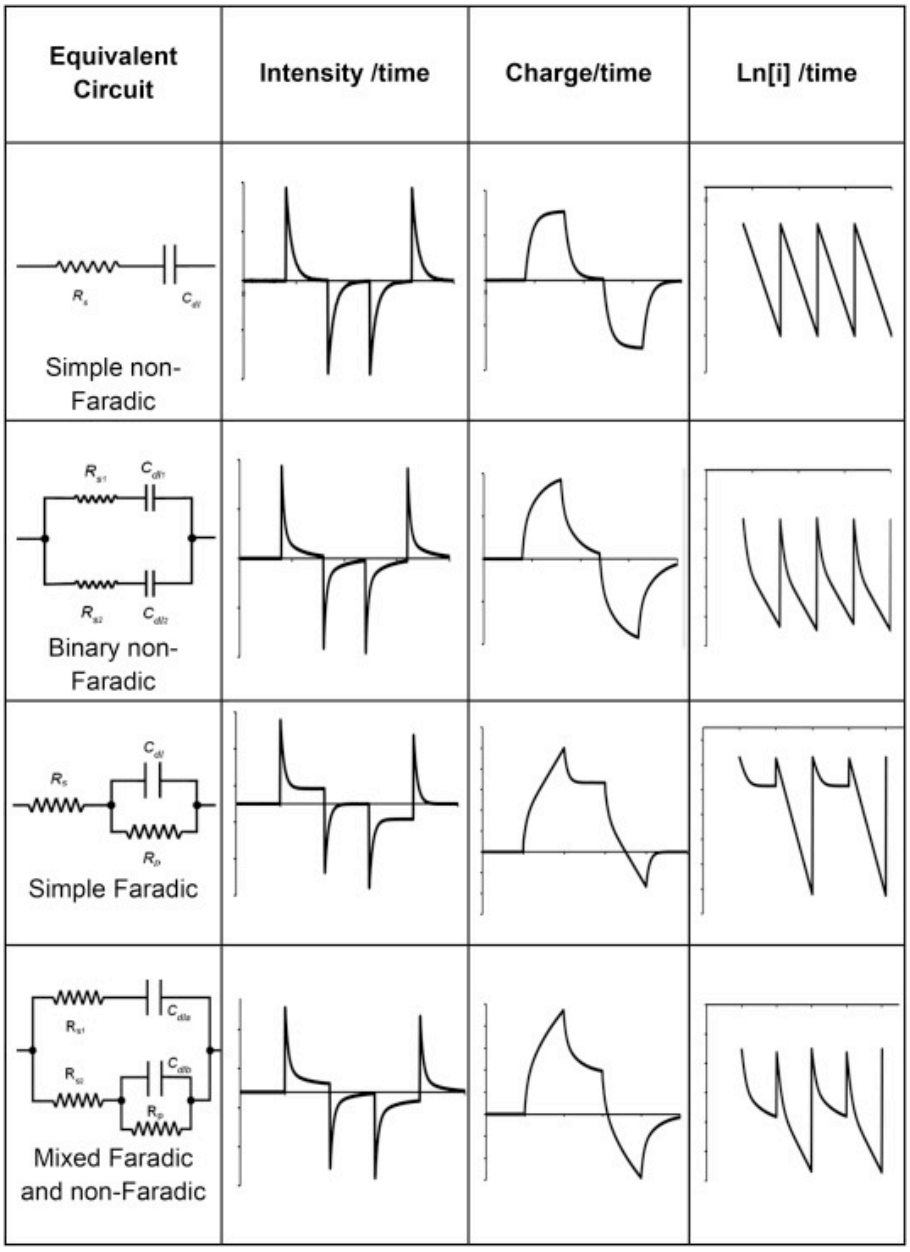

Figure 16. Intensity-time, charge-time, and logarithm of the absolute value of intensity versus time responses for the same equivalent circuits.

Therefore, the response of a real electrochemical system to the proposed potential steps sequence can be used to identify the equivalent circuit that models the behavior of this system by means of a visual inspection of the log(i(t)) curve. Once the equivalent circuit has been identified, the algebraic expression of the accumulated charge for this EC can be employed to experimentally determine the values of the double layer capacitance (C_{dl}), the solution resistance (R_s), and the polarization resistance of the redox process (R_p).

5. Conclusions

We have proposed electric equivalent circuits to model different Faradaic and non-Faradaic electrochemical systems and have designed a potential pulse sequence in order to analyze the behavior of these ECs. The sequence has been conceived as a cycle so that a situation of null total accumulated charge is achieved when the time and amplitude parameters are appropriate. This allows electrochemical studies of the system to be performed with very low induced perturbation values. The algebraic expressions of the current and accumulated charge for each EC when this potential step sequence is applied have been obtained and validated with experimental measurements. A very good fitting was observed between the theoretical values and the experimental data for the accumulated charge.

The morphology of the logarithm of the current versus time plot allows us to identify the different types of ECs. Hence, applying the proposed potential step

sequence to a real electrochemical system would enable the identification of an EC corresponding to the processes taking place in the system. Besides, the algebraic expression of the accumulated charge corresponding to the identified EC can be used to obtain the values of relevant parameters of the electrochemical system such as the double layer capacitance, the solution resistance, and the polarization resistance of the redox process.

In the second part of this study, reversible electrochemical systems are evaluated using the proposed potential pulse signal and the validity of the described method is analyzed.

6. Acknowledgments

Financial support from the Spanish Government (FEDER project BIA2016-78460-C3-3-R, MAT2015-64139-C4-3-R and RTI2018-100910-B-C43 (MINECO/FEDER) projects) is gratefully acknowledged. The predoctoral scholarships granted to Ana Martínez Ibernón (FPU 16/00723) and to José Enrique Ramón Zamora within the program ‘‘Formación de Profesorado Universitario’’ from the Ministry of Education, Culture and Sport (FPU 13/00911) are also gratefully acknowledged.

7. Bibliography

[1] A.K. Deisingh, D.C. Stone, M. Thompson, Applications of electronic noses and tongues in food analysis, Int. J. Food Sci. Technol. 39 (2004) 587–604.

doi:10.1111/j.1365-2621.2004.00821.x.

[2] J. Olsson, F. Winquist, I. Lundström, A self polishing electronic tongue, Sensors Actuators B Chem. 118 (2006) 461–465. doi:10.1016/J.SNB.2006.04.042.

[3] C. Krantz-Rülcker, M. Stenberg, F. Winquist, I. Lundström, Electronic tongues for environmental monitoring based on sensor arrays and pattern recognition: a review, Anal. Chim. Acta. 426 (2001) 217–226. doi:10.1016/S0003-2670(00)00873-4.

[4] M. Gattrell, N. Gupta, A. Co, A review of the aqueous electrochemical reduction of CO2 to hydrocarbons at copper, J. Electroanal. Chem. 594 (2006) 1–19. doi:10.1016/J.JELECHEM.2006.05.013.

[5] D. Henderson, S. Lamperski, Simple Description of the Capacitance of the Double Layer of a High Concentration Electrolyte, J. Chem. Eng. Data. 56 (2011) 1204–1208. doi:10.1021/je101106z.

[6] M. Breiter, M. Kleinerman, P. Delahay, Structure of the Double Layer and Electrode Processes, J. Am. Chem. Soc. 80 (1958) 5111–5117. doi:10.1021/ja01552a029.

[7] M.A. V. Devanathan, B.V.K.S.R.A. Tilak, The Structure of the Electrical Double Layer at the Metal-Solution Interface, Chem. Rev. 65 (1965) 635–684. doi:10.1021/cr60238a002.

[8] R. Parsons, The electrical double layer: recent experimental and theoretical developments, Chem. Rev. 90 (1990) 813–826. doi:10.1021/cr00103a008.

[9] W. Schmickler, Electronic Effects in the Electric Double Layer, Chem. Rev. 96 (1996) 3177–3200. doi:10.1021/CR940408C.

[10] A.J. Bard, L.R. Faulkner, Electrochemical methods : fundamentals and

applications, Wiley, 2001. https://www.wiley.com/en-us/Electrochemical+Methods%3A+Fundamentals+and+Applications%2C+2nd+Edition-p-9780471043720 (accessed November 15, 2018).

[11] J.-S. Filhol, M. Neurock, Elucidation of the Electrochemical Activation of Water over Pd by First Principles, Angew. Chemie Int. Ed. 45 (2006) 402–406. doi:10.1002/anie.200502540.

[12] J.A. Santana, C.R. Cabrera, Y. Ishikawa, A density-functional theory study of electrochemical adsorption of sulfuric acid anions on Pt(111), Phys. Chem. Chem. Phys. 12 (2010) 9526. doi:10.1039/c000981d.

[13] R. Bataller, J.M. Gandía, E. García-Breijo, M. Alcañiz, J. Soto, A study of the importance of the cell geometry in non-Faradaic systems. A new definition of the cell constant for conductivity measurement, Electrochim. Acta. 153 (2015) 263–272. doi:10.1016/j.electacta.2014.12.014.

[14] M.C. Martínez-Bisbal, E. Loeff, E. Olivas, N. Carbó, F.J. García-Castillo, J. López-Carrero, I. Tormos, F.J. Tejadillos, J.G. Berlanga, R. Martínez-Máñez, M. Alcañiz, J. Soto, A Voltammetric Electronic Tongue for the Quantitative Analysis of Quality Parameters in Wastewater, Electroanalysis. 29 (2017) 1147–1153. doi:10.1002/elan.201600717.

[15] S. Kumar, A. Ghosh, B. Tudu, R. Bandyopadhyay, A circuit model estimation of voltammetric taste measurement system for black tea, Meas. J. Int. Meas. Confed. (2019). doi:10.1016/j.measurement.2019.03.076.

[16] I. Campos, M. Alcañiz, R. Masot, J. Soto, R. Martínez-Máñez, J.-L. Vivancos, L. Gil, A method of pulse array design for voltammetric electronic tongues, Sensors Actuators B Chem. 161 (2012) 556–563. doi:10.1016/J.SNB.2011.10.075.

[17] E. Barsoukov, J.R. Macdonald, Impedance Spectroscopy: Theory, Experiment, and Applications, John Wiley & Sons, Inc., Hoboken, NJ, USA, 2005. doi:10.1002/0471716243.

[18] L.-H.L. Miaw, S.P. Perone, Theoretical and experimental studies of the effects of charging currents in potential-step voltammetry, Anal. Chem. 51 (1979) 1645–1650. doi:10.1021/ac50047a015.

APPENDIX: Response of equivalent circuits

This appendix contains the derivations of the responses of all equivalent circuits presented before a potential step. Unless otherwise stated, the following equations refer to times after t_1 in Fig. 1, that is, they model the response to the first potential step. Given the linearity of these electrical models, the responses to all subsequent steps can be modeled as time-delayed versions of the response to the first step, multiplied by a constant. Note that, according to Fig. 2, the potential applied to the linear circuit model equals the potential applied to the overall electrochemical system $v(t)$, with the waveform depicted in Fig. 1, minus the OCP V_0.

I. RC circuit

Considering the circuit in Fig. 5B, the voltage at the resistor is:

$$v_R = R_s i_{\mathrm{NF}} \qquad \text{(A.1)}$$

where the time dependence of current i_{NF} and voltage v_R has not been made explicit for simplicity. The voltage-to-current relation at the capacitor is given by:

$$i_{\mathrm{NF}} = C_{\mathrm{dl}} \frac{\partial v_C}{\partial t} \tag{A.2}$$

Since the resistor and capacitor are connected in series:

$$v - V_0 = v_R + v_C \tag{A.3}$$

Considering the three previous equations:

$$v - V_0 = R_s i_{\mathrm{NF}} + v_C = R_s C_{\mathrm{dl}} \frac{\partial v_C}{\partial t} + v_C \tag{A.4}$$

Therefore, the differential equation that describes the behavior of the circuit in Fig. 5B as a result of the first voltage step ($t_1 < t$) is:

$$V_1 - V_0 = R_{\mathrm{s}} C_{\mathrm{dl}} \frac{\partial v_C}{\partial t} + v_C \tag{A.5}$$

with the initial condition:

$$v_C(t \leq t_1) = 0 \tag{A.6}$$

The solution to Eq. A.5 is:

$$v_C(t) = (V_1 - V_0)\left(1 - e^{-\frac{t-t_1}{R_s C_{dl}}}\right) = \Delta V_1 \left(1 - e^{-\frac{t-t_1}{R_s C_{dl}}}\right) \quad \text{(A.7)}$$

Considering Eq. A.2:

$$i_1 = i_{NF} = C_{dl}\frac{\partial v_C}{\partial t} = \Delta V_1 C_{dl}\frac{\partial}{\partial t}\left(1 - e^{-\frac{t-t_1}{R_s C_{dl}}}\right) = \frac{\Delta V_1}{R_s} e^{-\frac{t-t_1}{R_s C_{dl}}} \quad \text{(A.8)}$$

The overall current resulting from the effect of all voltage steps applied before time *t* can thus be obtained as:

$$i_j = \sum_{i=1}^{j} \frac{\Delta V_i}{R_s} e^{-\frac{t-t_i}{R_s C_{dl}}} \qquad t_j < t \leq t_{j+1} \quad \text{(A.9)}$$

Note that all the additive terms in (A.9) vanish with time. In fact, if the duration of voltage steps is sufficiently greater than the time constant of the circuit $\left(\Delta t = t_{j+1} - t_j \gg R_s C_{dl}\right)$, then the current i_j can be approximated by:

$$i_j \approx \frac{\Delta V_j}{R_s} e^{-\frac{t-t_j}{R_s C_{dl}}} \qquad t_j < t \leq t_{j+1} \quad \text{(A.10)}$$

That is, the current intensity of this non-Faradaic branch depends on the last voltage step, as indicated by Eq. 3.

II. RC circuit with a resistor in parallel with the capacitor

Considering the circuit in Fig. 9, the voltage at the resistor R_s is:

$$v_{Rs} = R_s(i_{\mathrm{NF}} + i_{\mathrm{F}}) \tag{A.11}$$

The voltage-to-current relationship at the capacitor is given by:

$$i_{\mathrm{NF}} = C_{\mathrm{dl}} \frac{\partial v_C}{\partial t} \tag{A.12}$$

And at the parallel resistor, it is:

$$v_{Rp} = R_p i_{\mathrm{F}} \tag{A.13}$$

Since $v_{Rp} = v_C$:

$$\frac{v_{Rs}}{R_s} = \frac{v_C}{R_p} + C_{\mathrm{dl}} \frac{\partial v_C}{\partial t} \tag{A.14}$$

Additionally:

$$v - V_0 = v_{Rs} + v_C \tag{A.15}$$

Therefore, the differential equation that describes the behavior of the circuit in Fig. 9 as a result of the first voltage step ($t > t_1$) is:

$$\frac{V_1 - V_0}{R_s} = C_{\mathrm{dl}} \frac{\partial v_C}{\partial t} + \left(\frac{1}{R_s} + \frac{1}{R_p}\right) v_C \tag{A.16}$$

with the initial condition:

$$v_C(t \le t_1) = 0 \tag{A.17}$$

The solution to Eq. A.16 with condition A.17 is:

$$v_C = (V_1 - V_0)\frac{R_p}{R_p + R_s}\left(1 - e^{-(t-t_1)\frac{R_p+R_s}{R_pR_sC_{\mathrm{dl}}}}\right) = \Delta V_1 \frac{R_p}{R_p + R_s}\left(1 - e^{-(t-t_1)\frac{R_p+R_s}{R_pR_sC_{\mathrm{dl}}}}\right) \tag{A.18}$$

Consequently, the expressions for branch currents are:

$$i_{\mathrm{NF}} = C_{\mathrm{dl}}\frac{\partial v_C}{\partial t} = \Delta V_1 \frac{C_{\mathrm{dl}}R_p}{R_p + R_s}\frac{\partial}{\partial t}\left(1 - e^{-(t-t_1)\frac{R_p+R_s}{R_pR_sC_{\mathrm{dl}}}}\right) = \frac{\Delta V_1}{R_s} e^{-(t-t_1)\frac{R_p+R_s}{R_pR_sC_{\mathrm{dl}}}} \tag{A.19}$$

$$i_{\mathrm{F}} = \frac{v_C}{R_p} = \frac{\Delta V_1}{R_p + R_s}\left(1 - e^{-(t-t_1)\frac{R_p+R_s}{R_pR_sC_{\mathrm{dl}}}}\right) \tag{A.20}$$

and the intensity of the total current through the electrochemical system:

$$i_1 = i_{\mathrm{F}} + i_{\mathrm{NF}} = \frac{\Delta V_1}{R_p + R_s}\left(1 - e^{-(t-t_1)\frac{R_p+R_s}{R_pR_sC_{\mathrm{dl}}}}\right) + \frac{\Delta V_1}{R_s} e^{-(t-t_1)\frac{R_p+R_s}{R_pR_sC_{\mathrm{dl}}}} \tag{A.21}$$

Note that, according to Eq. A.21, it may seem that the Faradaic component of the current is proportional to the potential step ΔV_1, and it has no direct dependence on the overpotential η_1, in contradiction to what is expressed in Eq. 3. However, if we build the solution for any time ($t_j < t < t_{j+1}$) as a linear combination of the time-delayed responses corresponding to each step[1], we get:

$$i_j = \sum_{i=1}^{j} \frac{\Delta V_i}{R_p + R_s}\left(1 - e^{-(t-t_i)\frac{R_p+R_s}{R_p R_s C_{\mathrm{dl}}}}\right) + \frac{\Delta V_i}{R_s} e^{-(t-t_i)\frac{R_p+R_s}{R_p R_s C_{\mathrm{dl}}}} \tag{A.22}$$

$$= \sum_{i=1}^{j} \frac{\Delta V_i}{R_p + R_s} + \sum_{i=1}^{j} \Delta V_i \left(\frac{1}{R_s} - \frac{1}{R_p + R_s}\right) e^{-(t-t_i)\frac{R_p+R_s}{R_p R_s C_{\mathrm{dl}}}}$$

The first term of the expression corresponds to the DC term of the resulting current, while the second one is a sum of exponentially decaying terms. The DC term can be simplified as:

$$\sum_{i=1}^{j} \frac{\Delta V_i}{R_p + R_s} = \sum_{i=1}^{j} \frac{V_j - V_{j-1}}{R_p + R_s} = \frac{V_j - V_0}{R_p + R_s} = \frac{\eta_j}{R_p + R_s} \tag{A.23}$$

Therefore, the amplitude of the DC term is proportional to the overpotential. As for the sum of exponentially decaying terms, if the duration of voltage steps is sufficiently greater than the time constant of the circuit $\left(\Delta t = t_j - t_{j-1} \gg \frac{R_p R_s C_{dl}}{R_p + R_s}\right)$, then all terms except for the last one can be neglected:

[1] This approach is based on the linearity of the system model.

$$i_j \approx \frac{\eta_j}{\mathrm{R_p} + \mathrm{R_s}} + \Delta V_j \left(\frac{1}{R_s} - \frac{1}{R_p + R_s} \right) e^{-(t-t_j)\frac{R_p + R_s}{R_p R_s C_{\mathrm{dl}}}} \quad \text{(A.24)}$$

where the constant term and the negative term in the parenthesis correspond to the Faradaic current i_F, and the positive term in the parenthesis corresponds to the non-Faradaic current i_{NF}. As indicated by Eq. 3, the non-Faradaic current mainly depends on the last voltage step, while its Faradaic counterpart depends on both the last voltage step and the overpotential.

III. Charge transferred across an RC circuit

The charge (q_j) stored in the capacitor (C_{dl}) of an RC circuit at any time between the j^{th} and $(j+1)^{th}$ voltage steps can be calculated by integrating Eq. A.9:

$$q_j = \sum_{i=1}^{j} \int_{t_i}^{t} \frac{\Delta V_i}{R_s} e^{-\frac{\tau - t_i}{R_s C_{\mathrm{dl}}}} \mathrm{d}\tau = -\sum_{i=1}^{j} \Delta V_i C_{\mathrm{dl}} \left(e^{-\frac{\tau - t_i}{R_s C_{\mathrm{dl}}}} \right)_{t_i}^{t} = \quad \text{(A.25)}$$

$$= C_{\mathrm{dl}} \sum_{i=1}^{j} \Delta V_i \left(1 - e^{-\frac{t - t_i}{R_s C_{\mathrm{dl}}}} \right)$$

Note that this expression can be decomposed as the sum of a constant plus an exponentially decaying term:

$$q_j = C_{\mathrm{dl}} \sum_{i=1}^{j} \Delta V_i - C_{\mathrm{dl}} \sum_{i=1}^{j} \Delta V_i e^{-\frac{t-t_i}{R_S C_{\mathrm{dl}}}} \tag{A.26}$$

$$= C_{\mathrm{dl}} \eta_j - C_{\mathrm{dl}} e^{-\frac{t-t_j}{R_S C_{\mathrm{dl}}}} \sum_{i=1}^{j} \Delta V_i e^{-\frac{t_j-t_i}{R_S C_{\mathrm{dl}}}}$$

And, for long enough voltage steps $\left(\Delta t = t_{j+1} - t_j \gg R_s C_{dl}\right)$:

$$q_j \approx C_{\mathrm{dl}} \eta_j - C_{\mathrm{dl}} \Delta V_j e^{-\frac{t-t_j}{R_S C_{\mathrm{dl}}}} \tag{A.27}$$

IV. Charge transferred across an RC circuit with a resistor in parallel with the capacitor

The total charge transferred across the circuit in Fig. 9 for times $t_j < t < t_{j+1}$ can be obtained by integration of Eq. A.22:

$$q_j = \int_{t_1}^{t} \left(\sum_{i=1}^{j} \frac{\Delta V_i}{R_p + R_s} + \sum_{i=1}^{j} \Delta V_i \left(\frac{1}{R_s} - \frac{1}{R_p + R_s} \right) e^{-(\tau - t_i)\frac{R_p + R_s}{R_p R_S C_{\mathrm{dl}}}} \right) \mathrm{d}\tau \tag{A.28}$$

$$= \sum_{i=1}^{j} \int_{t_i}^{t} \frac{\Delta V_i}{R_p + R_s} \mathrm{d}\tau$$

$$+ \sum_{i=1}^{j} \Delta V_i \frac{R_p}{R_s\left(R_p + R_s\right)} \int_{t_i}^{t} e^{-(\tau - t_i)\frac{R_p + R_s}{R_p R_S C_{\mathrm{dl}}}} \mathrm{d}\tau$$

$$= \sum_{i=1}^{j} \frac{\Delta V_i (t - t_i)}{R_p + R_s} + \sum_{i=1}^{j} \frac{\Delta V_i R_p^2 C_{\mathrm{dl}}}{\left(R_p + R_s\right)^2} \left(1 - e^{-(t-t_i)\frac{R_p + R_s}{R_p R_S C_{\mathrm{dl}}}} \right)$$

Note that the numerator of the first term is the integral of the voltage (compare the expression to the graph in Figure 1). It can also be expressed as a function of the overpotentials and the step duration Δt:

$$q_j = \frac{\eta_j\left(t - t_j\right)}{R_p + R_s} + \frac{\Delta\, t}{R_p + R_s}\sum_{i=1}^{j-1}\eta_i + \sum_{i=1}^{j}\frac{\Delta V_i R_p^2 C_{\mathrm{dl}}}{\left(R_p + R_s\right)^2}\left(1 - e^{-(t-t_i)\frac{R_p+R_s}{R_p R_s C_{\mathrm{dl}}}}\right) \tag{A.29}$$

For long step durations ($\left(\Delta t \gg \frac{R_p R_s C_{\mathrm{dl}}}{R_p+R_s}\right)$ Eq. A.29 can be simplified:

$$q_j = \frac{\eta_j\left(t - t_j\right)}{R_p + R_s} + \frac{\Delta\, t}{R_p + R_s}\sum_{i=1}^{j-1}\eta_i + \frac{\eta_j R_p^2 C_{\mathrm{dl}}}{\left(R_p + R_s\right)^2} - \frac{\Delta V_j R_p^2 C_{\mathrm{dl}}}{\left(R_p + R_s\right)^2} e^{-(t-t_j)\frac{R_p+R_s}{R_p R_s C_{\mathrm{dl}}}} \tag{A.30}$$